FOLIA OECOLOGICA – vol. 52, no. 1 (2025), doi: 10.2478/foecol-2025-0003

Spring phenological models combining the effects of temperature and photoperiod are successfully transferred to various spatial and temporal scales: a case study of *Aesculus hippocastanum* L.

Svetlana Korsakova[1,3*], Pavel Korsakov[1,2], Vladislav Evstigneev[3]

[1]Nikitsky Botanical Gardens—National Scientific Center of the RAS, 298648 Yalta, Russia
[2]Crimean Department of Hydrometeorology and Environmental Monitoring, 298648 Yalta, Russia
[3]Laboratory of Regional Climate Systems, Sevastopol State University, 299053 Sevastopol, Russia

Abstract

Korsakova, S., Korsakov, P., Evstigneev, V., 2025. Spring phenological models combining the effects of temperature and photoperiod are successfully transferred to various spatial and temporal scales: a case study of *Aesculus hippocastanum* L. *Folia Oecologica*, 52 (1): 22–33.

On the basis of long-term, high-quality in situ observations on phenological and meteorological data, we parameterised and examined the performances of four single-phase and two two-phase models for the prediction of the leaf unfolding and flowering dates of horse chestnut (*Aesculus hippocastanum* L.). Amongst models, those combining the effects of temperature and photoperiod showed the best phenophase prediction, suggesting the influence of photoperiod on the leaf unfolding and flowering of *A. hippocastanum*. The obtained coefficients showed that the effect of photoperiod was greater on leaf unfolding than on flowering. Comprehensive assessment revealed that the single-phase BCdoy model demonstrated the best fitting for both phenophases. This model also showed sufficiently high accuracy and the transferability of results in time and space. The proposed models can be used to predict the spring phenophases of *A. hippocastanum* in European and Asian countries, where this ornamental tree species is widely used in urban landscaping, and to optimise control methods against *Cameraria ohridella* Deschka & Dimić (Lepidoptera, Gracillariidae). For *C. ohridella*, the first flying out of adults after overwintering begins at the onset of horse chestnut leaf unfolding and mass flight occurs during the full flowering period.

Keywords

climate change, flowering time, leaf miner, leaf unfolding, photosensitivity, temperature

Introduction

Phenology is attracting increasing interest from scientists around the world due to its sensitivity to climatic changes (Minin et al., 2016; Mo et al., 2023). Variations in the timing of phenological phase onset in plants have effects on ecosystem processes, such as photosynthesis, carbon and water cycles, biomass accumulation, microclimate, animal–plant interactions (Richardson et al., 2013) and competition for light and water resources. Therefore, the importance of the study of phenological phase changes over the long term has increased in light of the effects of climate warming on the plant and animal worlds.

In plants, flowering and leaf unfolding are the key phenological phases that determine their reproduction and growth (Wang et al., 2022). For most deciduous trees of the Northern Hemisphere, these phases occur in spring (Buonaiuto and Wolkovich, 2021). Temperature is the most important abiotic factor affecting plant development in spring amongst (Parmesan, 2007; Flynn and Wolkovich, 2018). The timing of vegetation initiation in approximately 30% of plant species (Zohner et al., 2016)

*Corresponding author:
e-mail: korsakova2002@mail.ru

is controlled by photoperiod and temperatures (Laube et al., 2014; Gauzere et al., 2019). Although the influence of photoperiod as the main factor for spring development is disputed, its importance may increase due to global warming (Malyshev et al., 2018). For example, a shortened photoperiod may reduce temperature sensitivity and increase the need for warmth to restrain the excessively early phenological development of a species (Fu et al., 2019).

The associated roles of winter cooling, spring warming and photoperiod in regulating the timing of spring phenophases of plants are closely related to the ecological characteristics of a species (Polgar and Primack, 2011; Basler and Körner, 2012; Laube et al., 2014; Zohner and Renner, 2015). During winter, plant buds undergo three different dormancy states: para-, endo- and ecodormancy (Lang et al., 1987). The paradormancy phase is induced by physiological factors outside the plant bud. The endodormancy phase, which is induced by internal causes, has adaptive importance and is a hereditarily fixed state that persists even when growth-favourable external conditions occur. In the ecodormancy phase, growth inhibition is induced by the absence of favourable environmental conditions for growth processes. Once favourable conditions for growth are established, ecodormancy releases (Lang et al., 1987; Basler, 2016).

The analysis and prediction of plant phenological reactions to climatic changes of varying intensities are given a special role because changes in plant life can substantially affect individual ecosystem components and the entire ecosystem (Wolkovich et al., 2012). Phenological models based on physiological processes are used to quantify the influence of environmental factors on the seasonal development of plants. They differ in their levels of complexity and types of response functions to environmental conditions (Basler, 2016). Models that describe the cumulative effect of temperature on bud development during the ecodormancy phase are called one-phase models. Complex two-phase models account for the chilling and forcing temperatures affecting bud development during the endo- and ecodormancy phases (Basler, 2016; Mo et al., 2023). As the number of factors increases, the complexity of models and their parameterisation also increases. Given the lack of a single universal model for predicting the dates of phenophases in spring for different plant species, the best predictive models are still species-specific (Basler, 2016). Few studies comparing their performances and reliability exist (Basler, 2016). Performance refers to the ability of a model to provide accurate predictions under the conditions used to calibrate it, and reliability refers to the ability of a model to provide accurate predictions under varying external conditions (Asse et al., 2020). Therefore, comparing the performance and reliability of one- and two-phase models under climate change can be highly useful.

Currently, testing, comparing the performances of phenological models and predicting the phenological responses of plants to climate change under different warming scenarios is predominantly conducted in Europe and China (Wolkovich et al., 2012; Zohner et al., 2016; Basler, 2016; Gauzere et al., 2019; Asse et al., 2020; Wang et al., 2022; Mo et al., 2023). This situation is greatly facilitated by the availability of open-access science and educational phenological observation databases, such as Pan European Phenological database (http://www.pep725.eu) and Chinese Phenological Observation Network (http://www.cpon.ac.cn/) (GE et al., 2015).

Russian phenological data, which have a history of secular observations on the seasonal development of plant species, are unique and important for science. Despite the active accumulation of phenological knowledge and contributions of leading scientists to the development of phenological methodology, only a small part of the phenological heritage in Russia is currently available for scientific analysis (Minin et al., 2020). "Chronicles of Nature Calendar," a long-term and large-scale multitaxon database on phenological and climatic observations collected in the Russian Federation, Ukraine, Uzbekistan, Belarus and Kyrgyzstan, has been published recently (Ovaskainen et al., 2020) and is freely available (http://chronicleofnature.com/). However, as of today, only approximately 5% of the total phenological data have been digitised, and the majority of the data are unavailable to the public domain (Minin et al., 2020).

Therefore, quantifying the relationship between the environment and plant functional traits and accurately predicting phenological changes are important for understanding and forecasting the effects of climate change. This relationship is best revealed through detailed long-term observations on organisms in the same system.

We focused our analysis on horse chestnut (*Aesculus hippocastanum* L.), a large deciduous tree, because this species is widespread in tree plantations, gardens and streets across Europe and other temperate regions. It is extensively utilised in similar studies in European countries wherein contradictory results have been obtained regarding its phenological responses to photoperiod (Basler and Körner, 2012; Laube et al., 2014; Zohner and Renner, 2015; Fu et al., 2019; Geng et al., 2022). Recently, horse chestnut trees in almost all regions of their distribution have been affected by the horse chestnut leaf miner moth, *Cameraria ohridella* Deschka & Dimić, 1986 (Lepidoptera, Gracillariidae). This situation not only leads to the loss of the trees' decorative appeal but also weakens them, thereby reducing their resistance to adverse environmental factors. For *C. ohridella*, the flying out of adults after overwintering begins at the leaf unfolding onset of horse chestnut in spring (Korzh and Trikoz, 2022), and their mass flight occurs during the full flowering period (Shvydenko et al., 2021). Therefore, the accurate prediction of the leaf unfolding and flowering dates of horse chestnut is of great importance in the development of effective measures to optimise pest control methods.

The goals of this study are based on detailed observations over an extended period of time and are as follows: (1) to compare the performance of parameterised phenological models for the leaf unfolding and flowering of horse chestnut; (2) to find the optimal phenological model for each phenophase; (3) and to test selected models for

spatial and temporal transferability by using a set of phenological and meteorological data covering a wide range of latitudes, longitudes and altitudes above sea level.

Materials and methods

Phenological and climatic data

We used high-quality phenological (provided by uniform methodology and observations by experienced specialists over the entire period and at the same sites) and meteorological data collected over a long period (1931–2022) from Nikitsky Sad agrometeorological station to parameterise the models for the first leaf unfolding and full flowering of *A. hippocastanum*. Study sites for phenological observations are located in the area of the Nikitsky Botanical Garden (Yalta region, 44.51°N, 34.24°E, altitude of 190 m above sea level) in the northern part of the Black Sea region in the territory of the Southern Coast of Crimea (SCC). The agrometeorological station Nikitsky Sad is located in the vicinity (approximately 200 m) of the sites of phenological observations. Using the long-term and homogeneous dataset of observations favours the identification of only climate-induced changes in the flora regime in the area.

The climate of the SCC is classified as subtropical Mediterranean with hot arid summers, predominance of autumn–winter precipitation and mild wet winters with frequent thaws. Throughout the year, the average monthly air temperatures are above 0 °C, with February being the coldest month and August being the warmest. The average annual air temperature is 12.6 °C, and the average annual precipitation is 592 mm (Korsakova et al., 2023).

The date of phenophase onset was considered to be the day of phenophase onset in at least 50% of plants. Phenological observations were made on 5–10 horse chestnut trees once every 2 days during spring development. Two phenological stages based on the Biologische Bundesantalt, Bundessortenamt and Chemische Industrie (BBCH) code were considered in this study: BBCH 11, leaf unfolding and BBCH 65, full flowering onset (Finn et al., 2007).

Phenological models

We tested six phenological models (Table S1), which differed by their complexities and types of response functions to environmental signals (temperature and photoperiod): GDD, BCdoy, SIGdoy, SIGFOTOdoy, SEQBCdoy and UniChill (Olsson et al., 2017; Korsakova et al., 2020). The GDD model (Chuine et al., 2003) describes the linear response of plants to temperatures above the base temperature (Tb) as a parameter. The BCdoy model (Blümel and Chmielewski, 2012) is a modified extension of the GDD model with a parameterised starting day of heat accumulation (forcing temperature), supplemented by an exponential constant (*EXPO*) to relate the photoperiod and temperature response. In the SIGdoy (Migliavacca et al., 2012), SIGFOTOdoy (Korsakova et al., 2023) and UniChill (Chuine, 2000) models, the response of phenological processes to temperature is described by a sigmoidal function starting from a parameterised day. In the SEQBCdoy model, the daily rate of chilling (*Rc*) is described by a triangular function (Hänninen, 1990), and the linear BCdoy describes the forcing level (Blümel and Chmielewski, 2012).

While modelling, we adhered to the assumption that the date of bud emergence from dormancy (*t1*) occurs after the accumulation of the daily rate of chilling (*Rc*) reaches a critical sum of chilling units C^* (see Eqn.1):

$$Sc_t = \sum_{t0}^{t1} Rc\,(Tt) \geq C^*, \quad (1)$$

where Sc_t is the state of chilling; *Rc* is the daily rate of chilling; *t0* is the starting date of chilling unit accumulation (day of the year [DOY]); *t1* is the date of the end of the endodormancy phase (the chilling requirement is completed, start of forcing) (DOY); *Tt* is the daily mean air temperature (°C); and C^* is the chilling unit requirement for endodormancy release (CU).

In two-phase sequential models, *t1* is the starting

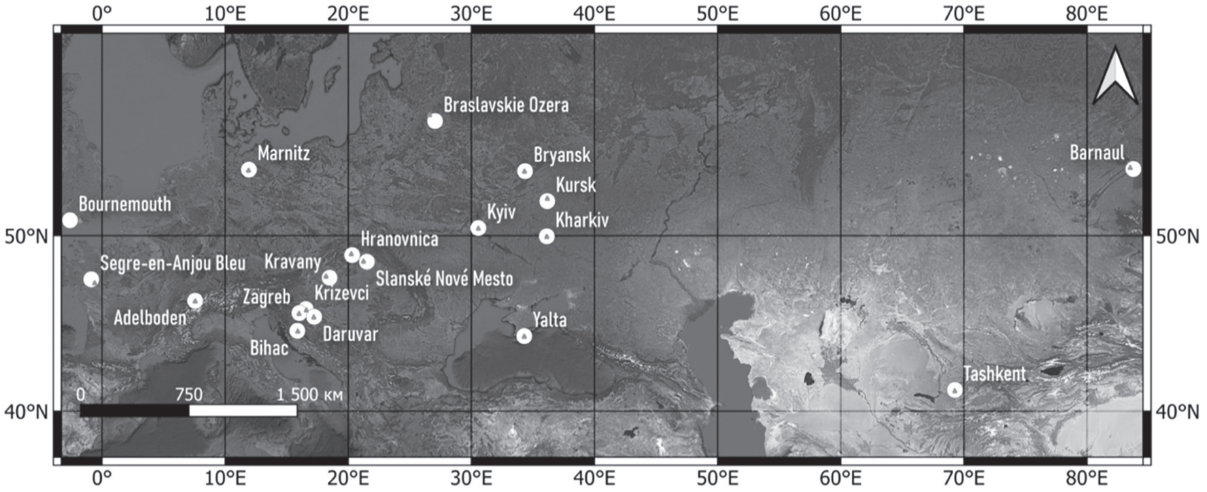

Fig. 1. Distribution of the phenological and weather stations used in this study. Circles indicate phenological stations, and triangles indicate meteorological stations.

date of forcing accumulation. In the single-phase external forcing models GDD, BCdoy, SIGdoy and SIGFOTOdoy (Table S1), it is assumed that at time t_1, the demand for low-temperature forcing is fulfilled or the plant does not require vernalisation (Chuine et al., 2003).

The duration of forcing accumulation from t1 to the date of phenophase onset (t_2) is related to the temperature sums of forcing (*Sf*) and accumulated daily rates of forcing (*Rf*). Phenophase occurs when the accumulated Rf reaches a critical amount of forcing units F^* (Eqn. 2):

$$Sf_t = \sum_{t1}^{t2} Rf(Tt) \geq F^*, \quad (2)$$

where Sf_t is the state of forcing; *Rf* is the daily rate of forcing; *t1* and *t2* are the dates of the start of temperature forcing and phenophase onset, respectively (DOY); Tt is the daily mean air temperature (°C); and F^* is the critical amount of forcing units needed to reach phenophase onset (FU).

The input data for modelling were the daily mean air temperatures and photoperiod duration. The duration of day length was calculated as a function of latitude and DOY (Forsythe et al., 1995). The parameters of phenological models were selected through evolutionary optimisation by using the Microsoft Excel add-in "Solution Search" (Korsakova et al., 2023). The optimisation goal function was the root mean square error (RMSE) expressed in days to minimise the difference between the forecast and observation dates. The optimisation procedure was repeated at least 30 times to ensure that the global optimum was reached. This iterative process was continued until the value of the objective function (minimisation of RMSE) stabilised, that is, it ceased to change over several consecutive calculations with a precision of up to $1e^{-15}$ due to Excel's limitation on the number of significant digits that could be displayed. The phenological models were verified by using data from odd-numbered years, and data from even-numbered years were used for validation. The best models selected were additionally tested for spatial and temporal transferability.

Freely available data from the Pan-European Phenology Project (PEP) (http://www.pep725.eu) (Templ, 2018) and recent studies were used to test phenological models (Fazilova, 2013; Kuranda, 2021; Ovaskainen et al., 2020; Shvydenko et al., 2021). Data on daily mean temperature from the nearest meteorological stations were obtained from the All-Russia Research Institute of Hydrometeorological Information–World Data Centre, Roshydromet (http://meteo.ru/data), Global Weather Data Portal (https://rp5.ru) and WMO/King Meteorological Institute (Netherlands) (https://climexp.knmi.nl/). The phenological and meteorological datasets used for model validation cover-ed wide ranges of latitudes (from 41.27°N to 55.87°N), longitudes (from −1.88°E to 83.78°E) and elevations (from 11 m to 1350 m) (Fig. 1, Tables S2 and S3).

Model estimation

The comparative assessment of model accuracies was performed on the basis of four goodness-of-fit measures:

Table 1. Best parameter sets and statistics (R^2, RMSE, AIC, and θ) of the phenology models used to predict the leaf unfolding dates of *A. hippocastanum*

Phenological model					
GDD	BCdoy	SIGdoy	SIGFOTOdoy	SEQBCdoy	UniChill
Parameters					
t_1 = 1.Jan T_b = 6.7 F^* = 85.0	t_1 = 28.Jan T_b = 2.2 *EXPO* = 3.4781 F^* = 549.1	t_1 = 14.Feb b_f = −0.1533 c_f = 13.9044 F^* = 14.7	t_1 = 13.Feb b_f = −0.4768 c_f = 6.9606 *EXPO* = 1.7976 F^* = 36.4	t_0 = 01.Nov T_{opt} = 2.5 C^* = 33.4 t_1 = 21.Feb T_b = 2.9 *EXPO* = 2.9485 F^* = 444.8	t_0 = 01.Dec a_c = 0.1000 b_c = −2.4404 c_c = −1.1483 C^* = 55.3 t_1 = 28. Jan b_f = −0.1970 c_f = 14.7879 F^* = 12.4
Goodness-of-fit measures of the calibration subset					
R^2 = 0.66 *RMSE* = 6.0 *AICc* = 128.78 θ = −0.3	R^2 = 0.80 *RMSE* = 3.5 *AICc* = 91.34 θ = 0.2	R^2 = 0.67 *RMSE* = 4.4 *AICc* = 108.36 θ = −0.4	R^2 = 0.71 *RMSE* = 4.2 *AICc* = 104.83 θ = −0.5	R^2 = 0.67 *RMSE* = 4.6 *AICc* = 112.1 θ = 0.4	R^2 = 0.65 *RMSE* = 5.1 *AICc* = 121.25 θ = 0.4
Goodness-of-fit measures of the validation subset					
R^2 = 0.62 *RMSE* = 7.0 θ = −0.7	R^2 = 0.60 *RMSE* = 4.7 θ = −1.4	R^2 = 0.53 *RMSE* = 5.3 θ = −1.6	R^2 = 0.60 *RMSE* = 4.9 θ = 0.7	R^2 = 0.61 *RMSE* = 4.9 θ = −1.7	R^2 = 0.60 *RMSE* = 5.6 θ = −2.3

t0, t1 and *t2*, starting dates of chilling, forcing unit accumulation and phenoevent onset, respectively. T_{opt}, optimal chilling temperature (°C). T_b, threshold of daily mean air temperature for forcing unit accumulation (°C). C^*, chilling unit requirement (CU). F*, forcing unit requirement (FU). a_c, b_c, c_c, b_f, c_f, empirical parameters of the sigmoidal function (c, chilling, f, forcing). *EXPO*, exponential constant for relating forcing accumulation to day length.

Table 2. Best parameter sets and statistics (R^2, RMSE, AIC and θ) of phenology models for predicting the dates of the full flowering onset of *A. hippocastanum*

GDD	BCdoy	SIGdoy	SIGFOTOdoy	SEQBCdoy	UniChill
Parameters					
t_1 = 1.Jan T_b = 6.8 F^* = 188.7	t_1 = 13.Feb T_b = 3.1 *EXPO* = 2.0282 F^* = 685.3	t_1 = 12.Feb b_f = −0.1314 c_f = 20.8575 F^* = 13.6	t_1 = 10.Feb b_f = −0.1901 c_f = 14.5597 *EXPO* = 1.0826 F^* = 26.3	t_0 = 01.Nov T_{opt} = 1.4 C^* = 45.1 t_1 = 12.Feb T_b = 5.4 *EXPO* = −0.01888 F^* = 247.5	t_0 = 01.Dec a_c = 0.1060 b_c = −2.0079 c_c = −4.4271 C^* = 72.9 t_1 = 13.Feb b_f = −0.1540 c_f = 19.5091 F^* = 12.9
Goodness-of-fit measures of the calibration subset					
R^2 = 0.70 *RMSE* = 4.2 *AICc* = 101.63 θ = −0.1	R^2 = 0.80 *RMSE* = 2.9 *AICc* = 70.57 θ = −0.1	R^2 = 0.83 *RMSE* = 2.7 *AICc* = 71.53 θ = −0.1	R^2 = 0.82 *RMSE* = 2.7 *AICc* = 72.86 θ = −0.2	R^2 = 0.81 *RMSE* = 3.3 *AICc* = 85.55 θ = −0.1	R^2 = 0.82 *RMSE* = 2.8 *AICc* = 76.60 θ = 0.0
Goodness-of-fit measures of the validation subset					
R^2 = 0.68 *RMSE* = 4.8 θ = 0.2	R^2 = 0.78 *RMSE* = 3.3 θ = 0.2	R^2 = 0.77 *RMSE* = 3.2 θ = 0.3	R^2 = 0.74 *RMSE* = 3.3 θ = 0.2	R^2 = 0.78 *RMSE* = 3.3 θ = 0.3	R^2 = 0.75 *RMSE* = 3.4 θ = 0.6

t0, *t1* and *t2*, starting dates of chilling, forcing unit accumulation and phenoevent onset, respectively. T_{opt}, optimal chilling temperature (°C). T_b, threshold of daily mean air temperature for forcing unit accumulation (°C). C^*, chilling unit requirement (CU). F^*, forcing unit requirement (FU). a_c, b_c, c_c, b_f, c_f, empirical parameters of the sigmoidal function (c, chilling, f, forcing). *EXPO*, exponential constant for relating forcing accumulation to day length.

coefficient of determination (R^2), RMSE (days), adjusted Akaike information criterion (*AICc*) and bias (θ, days):

$$R^2 = 1 - \frac{\sum_{i=1}^{n}(obs_i - pre_i)^2}{\sum_{i=1}^{n}(obs_i - \overline{obs_i})^2}, \quad (3)$$

$$RMSE = \sqrt{\frac{\sum_{i=1}^{n}(obs_i - pre_i)^2}{n}}, \quad (4)$$

$$AIC_C = n \cdot ln\left(\frac{\sum_{i=1}^{n}(obs_i - pre_i)^2}{n}\right) + 2 \cdot k + \left(\frac{2 \cdot k \cdot (k+1)}{n-k-1}\right), \quad (5)$$

$$\Theta = \frac{\sum_{i=1}^{n}(obs_i - pre_i)}{n}, \quad (6)$$

where obs_i is the observable date, obs_i is the observed mean date, pre_i is the predicted date of phenophase onset (in DOY), n is the number of years of observations and k is the number of model parameters (Gauzere et al., 2017; Korsakova et al., 2023).

Data analysis on modelling results was performed by using R software version 4.2.2 (R Core Team, 2022). Data visualisation and figures were created by using ggplot2 (Wickham, 2016).

Results

Reducing the uncertainty associated with the effect of climate change on natural systems requires the accurate assessment of vegetation feedback, which, in turn, depends on the accurate predictions of spring phenology and climate change. The parameters of single- and two-phase models were optimised on the basis of the data from long-term observations on the SCC (Tables 1–2) to select the most effective predictive model for the dates of the first leaf unfolding and full flowering onset of horse chestnut.

Residuals were tested for normality to assess the adequacy of the models (Fig. S1). In accordance with the results of the assessment, we can conclude that the analysed samples of the model residuals were normally distributed. Goodness-of-fit measures based on four criteria showed that all models satisfactorily described the winter–spring development of the generative structures of horse chestnut (Table 2). However, higher accuracy in approximating developmental processes to predict the timing of leaf unfolding was achieved when using the BCdoy, SIGFOTOdoy and SEQBCdoy models than when other models were applied (Table 1). Compared with those obtained by using the GDD, SIGdoy and UNIChill models, the RMSE values for the calculations of leaf unfolding date acquired by using these models were lower, differing insignificantly and ranging from 3.5 days to 4.9 days. The magnitude of systematic bias did not exceed 0.1–1.7 days, and the coefficients of determination ranged from 0.60 to 0.80. On the basis of the AIC measure, the best models for predicting the phenodates of leaf unfolding were determined to be BCdoy and SIGFOTOdoy and those for predicting the phenodates of full flowering onset were BCdoy, SIGdoy, SIGFOTOdoy, SEQBCdoy and UNIChill. Therefore, the

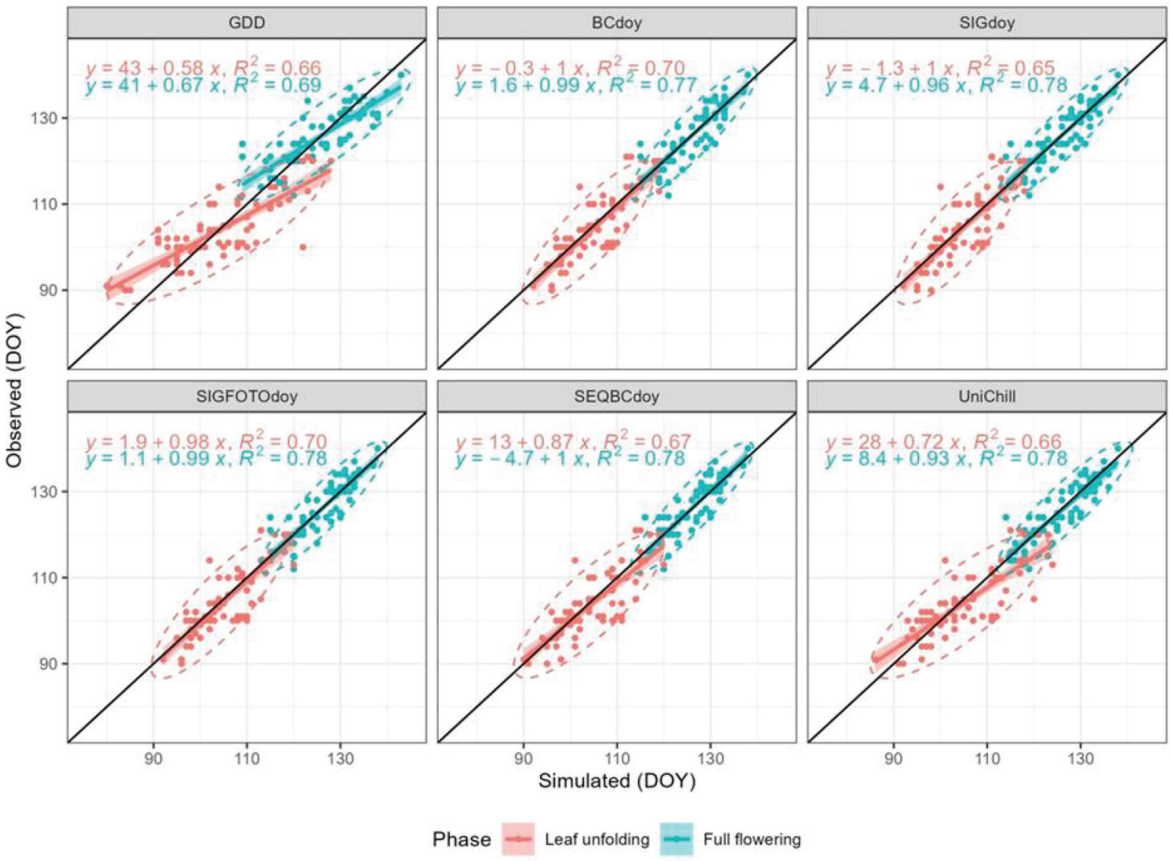

Fig. 2. Comparisons of the observed and model-predicted phenophase dates for *A. hippocastanum*. Simulated (x-axis) vs. observed (y-axis) dates in Julian days (DOYs) of leaf unfolding and full flowering. Dates of leaf unfolding are presented in pink, whereas those of full flowering are presented in blue.

interannual variability in the leaf unfolding and flowering dates of horse chestnut was better described by the models accounting for the combined effect of temperature and photoperiod on bud development processes (BCdoy, SIGdoy and SIGFOTOdoy) than by other models. Consistent with the data of earlier studies that showed strong photoperiodic control in the spring leaf unfolding of *A. hippocastanum* (Geng et al., 2022), the values of the obtained *EXPO* coefficients indicated that the influence of photoperiod was more significant for the leaf unfolding phase than for the flowering phase.

The degree of linear correspondence between the predicted and measured values was evaluated by regression analysis to identify the possible bias of the predicted leaf unfolding and flowering dates in accordance with phenological models towards systematic advance or delay (Fig. 2). The theoretically predicted value (y) and measured value (x) should have a linear relationship of 1:1.

The graphical analysis of the models revealed that the tangents of the linear regression slopes of most models, except for the GDD, SEQBCdoy and UNIChill models, for predicting the onset of phenological phases were close to unity for leaf unfolding. The shift parameters of BCdoy and SIGFOTOdoy were close to zero and did not exceed 1.9 days, indicating the absence of systematic error (Fig. 2). In general, the results of the comprehensive evaluation indicated that the best fit value for both phenophases was shown by the BCdoy model. The BCdoy model accurately described the interannual variability of leaf unfolding and full flowering and can be used to predict these phenophases.

Taking into account the trade-off between the expected accuracy and result transferability and the fact that phenological models tend to underestimate interannual variations in phenophases, the selected BCdoy model was further tested for transferability in time and space. For this purpose, data from independent observations of the leaf unfolding and full flowering of horse chestnut over a wide range of latitudes, longitudes and altitudes were used (Fig. 1, Table S2). These data were not used in model construction (Fig. 3).

The estimation of a single set of parameters for the BCdoy model to match phenological stages across all sites resulted in mean pooled external validation errors (RMSEs) of 5.6 days for the leaf unfolding phase and of 4.6 days for the flowering phase. In external validation across sites, the lowest RMSE for leaf unfolding were obtained in Marnitz, Germany (3.9 days), and the highest were obtained in Adelboden, Switzerland (7.6 days). The mean of the RMSE values for flowering ranged from 1.6 days in Bryansk (Russia) and 1.9 days in Daruvar (Croatia) to 7.5 days in Bournemouth (England).

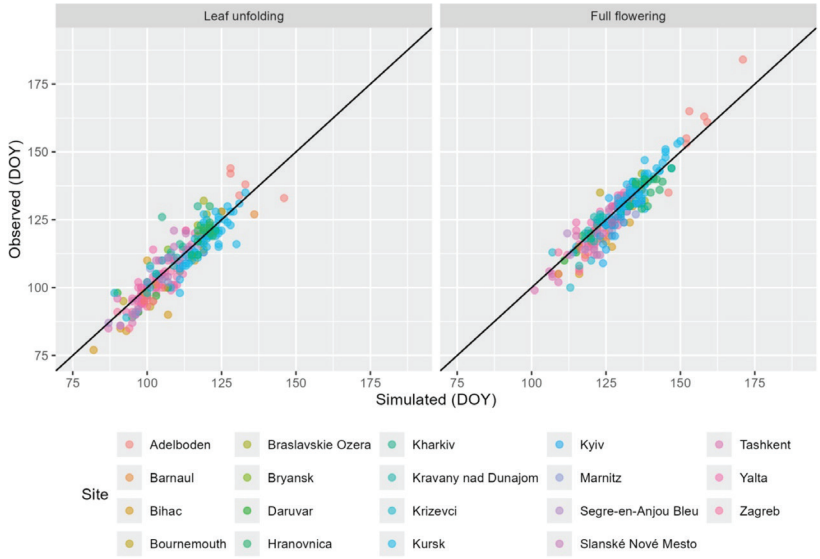

Fig. 3. Scatterplots of the observed and simulated leaf unfolding and flowering dates in a dataset for calibration (SCC, Yalta region) and independent verification (individual sites located in other regions) using the single-phase BCdoy model.

Discussion

Our study of six phenological models for predicting the leaf unfolding and flowering dates of *A. hippocastanum* based on long-term in situ data observations revealed that in general, the temperature-driven GDD model showed the lowest performance amongst the models that we tested. Moreover, the GDD model showed larger systematic biases than the other five models. Two-phase models (SEQBCdoy and UNIChill), with the exception of the GDD model, did not perform better than one-phase models. However, these models can simulate interannual variations in the date of the spring phenophase onset well. Some previous studies also showed that model complexity does not necessarily lead to increased accuracy, partly because not all species require chilling exposure (Basler, 2016; Meng, et al., 2021; Mo et al., 2023). From a statistical perspective, the two models for the prediction of leaf unfolding dates (BCdoy and SIGFOTOdoy) and the five models for the prediction of full flowering dates (BCdoy, SIGdoy, SIGFOTOdoy, SEQBCdoy and UNIChill) showed comparable predictive accuracy. In general, all models had higher accuracy in simulating full flowering dates than leaf unfolding dates.

A linear regression analysis–based comparison of the predicted and actual dates of the leaf unfolding and flowering onset of *A. hippocastanum* obtained by using the GDD and UNIChill models revealed significant bias. The tangent of the inclination angle of the linear regression models was less than one, and the shear ranged from 8 days to 28 days for the UNIChill model and from 41 days to 43 days for the GDD model. These results indicated that when calculated with these models, the onsets of leaf unfolding and flowering at early plant development in spring will be predicted with lag and those in a later period will be ahead of the real phenophase date. This situation may contribute to increasing uncertainty in transferring models to various spatial scales and in the long-term assessment of the effects of possible climate change (Korsakova et al., 2023).

Our results revealed that models including photoperiod demonstrated higher accuracy in the prediction of the spring phenology of horse chestnut and had better temporal transferability than other models. The superior phenophase prediction performance of the phenological models that included photoperiod to those that did not indicated that day length largely controlled the leaf unfolding and flowering days of *A. hippocastanum*. However, the coefficients obtained showed that the photoperiod effect was greater on leaf unfolding than on flowering. Our findings are at odds with some earlier published data (Basler and Körner, 2012) but align with several previous findings (Laube et al., 2014; Zohner et al., 2016; Flynn and Wolkovich, 2018; Geng et al., 2022) reflecting strong photoperiod control in spring leaf unfolding. Similar patterns regarding the effect of photoperiod on spring leaf-out were also revealed on the regional scale by using in situ observational datasets (Meng, et al., 2021).

According to the results of the comprehensive evaluation, the best fit value for both phenophases was shown by the single-phase BCdoy model. This model (model M1 in Blümel and Chmielewski, 2012; Basler, 2016; Mo et al., 2023) also provided the best results in modelling the timing of the spring phenology of horse chestnut and some other tree species in central Europe (Basler, 2016; Mo et al., 2023). Recent studies have demonstrated that single-phase heat–time models simulating only the ecodormancy phase often show similar or better performance than more complex two-phase models (Basler, 2016; Asse et all., 2020; Mo et al., 2023). The accuracy of predicting the onset of growth and flowering in spring largely depends on the structure of the phenological model, which requires an improved understanding of the interaction of various specific functional types of plants (photoperiod sensitivity and chilling requirement) with environmental factors (Chuine et al., 2003; Basler, 2016; Gauzere et al.,

2019; Meng et al., 2021).

The phenological observation sites used for BCdoy model validation in this study are located in Germany, Switzerland, England, France, Croatia, Slovakia, Bosnia and Herzegovina, Russia, Ukraine, Belarus and Uzbekistan, spanning elevations of 11–1,440 m above sea level, latitudes of 41.27°N–55.87°N and longitudes of 1.88°E–83.78°E. The transfer of the site-specific parameters of the BCdoy model for the SCC (Yalta region) to other sites with different climatic and geographical characteristics demonstrated the sufficiently high accuracy and transferability of the results in time and space in cool and warm regions. This finding allows the use of the BCdoy model to forecast the leaf unfolding and flowering dates of *A. hippocastanum* not only in the SCC but also in other regions where it is cultivated.

The model likely calculates plant development under current and warm climate conditions (Mo et al., 2023) realistically because the inclusion of day length limited the influence of temperature on bud development in the beginning of the year (Blümel and Chmielewski, 2012). A previous study (Meng et al., 2021) revealed the role of photoperiod as a critical factor regulating spring phenology, delaying early leaf unfolding and accelerating late leaf unfolding caused by temperature fluctuations. Thus far, however, many studies identified photoperiod as a critical but still understudied factor influencing spring phenology (Fu et al., 2019; Asse et al., 2020; Meng et al., 2021; Mo et al., 2023). Specifically, whether and to what extent day length affects phenological development is unclear, leading to considerable uncertainties in projecting future phenological changes (Meng et al., 2021).Therefore, the proposed models can be used to predict the spring phenophases of *A. hippocastanum* in European and Asian countries, where horse chestnut is widely used in urban landscaping and is one of the most valuable ornamental tree species. Currently, in almost all growing regions, the leaves of horse chestnut are damaged by the horse chestnut leaf miner *C. ohridella*. Given the devastating damage that it causes to horse chestnut in cities, *C. ohridella* is included in the list of the 100 most dangerous invasive species in the European Union (Korzh and Trikoz, 2022). A relationship has been found between the phenological development of horse chestnut and the life cycle of *C. ohridella* (Shvydenko et al., 2021; Korzh and Trikoz, 2022). After winter, moths begin to fly simultaneously with phenological indicators, such as the leaf unfolding onset of *A. hippocastanum* (Korzh and Trikoz, 2022), and their mass flight occurs at the full flowering of *A. hippocastanum* (Shvydenko et al., 2021). Our findings have considerable practical implications. Forecasting the spring phenophases of *A. hippocastanum* by using the developed phenological models will contribute to the optimisation of methods for controlling the horse chestnut leaf miner *C. ohridella* and the preservation of this popular ornamental tree.

Conclusions

We calibrated and examined six phenology models. The major parameters of these models were carefully estimated over local scales by using long-term meteorological data and phenological observations acquired *in situ*. All models performed better than the GDD model, and amongst models, the BCdoy model performed the best in the prediction of the leaf unfolding and flowering dates of *A. hippocastanum*. Our investigation provided evidence that the inclusion of the photoperiod effect in phenological models remarkably improves accuracy in predicting the temporal and spatial variations in the spring phenophases of leaf unfolding and flowering. The possibility of transferring a model that includes photoperiod to various spatial and temporal scales was successfully tested on the basis of independent observations for the leaf unfolding and flowering of horse chestnut over a wide range of latitudes, longitudes and altitudes above sea level. The phenological models for predicting the dates of leaf unfolding and flowering of *A. hippocastanum* developed in our study are useful tools for the control of *C. ohridella* because they offer valuable information for urban landscaping management and planning. In addition, the accurate prediction of phenological stages contributes to the implementation of effective strategies for controlling the number and reducing the harmfulness of phytophagous populations, as well as enabling timely action, to preserve the popular ornamental tree *A. hippocastanum*. Our findings point to the necessity of considering photoperiod together with temperature in predicting phenological changes under climate warming.

Acknowledgements

This study was conducted within the framework of the State Task № FNNS-2022-0003 of FSFIS "NBG-NSC" and of the programme "Prioritet-2030" of Sevastopol State University, Strategic Project #3 (Russian state assignment № 120090990063-3).

References

Asse, D., Randin, Ch.F., Bonhomme, M., Delestrade, A., Chuine, I., 2020. Process-based models outcompete correlative models in projecting spring phenology of trees in a future warmer climate. *Agricultural and Forest Meteorology*, 285–286: 107931. https://doi.org/10.1016/j.agrformet.2020.107931

Basler, D., 2016. Evaluating phenological models for the prediction of leaf-out dates in six temperate tree species across central Europe. *Agricultural and Forest Meteorology,* 217: 10–21. https://doi.org/10.1016/j.agrformet.2015.11.007

Basler, D., Körner, C., 2012. Photoperiod sensitivity of bud burst in 14 temperate forest tree species. *Agricultural and Forest Meteorology*, 165: 73–81. https://doi.org/10.1016/j.agrformet.2012.06.001

Blümel, K., Chmielewski, F.-M., 2012. Shortcomings of classical phenological forcing models and a way to overcome them. *Agricultural and Forest Meteorology*, 164: 10–19. https://doi.org/10.1016/j.agrformet.2012.

05.001

Buonaiuto, D.M., Wolkovich, E.M., 2021. Differences be tween flower and leaf phenological responses to environmental variation drive shifts in spring phenological sequences of temperate woody plants. *Journal of Ecology*, 109: 2922–2933. https://doi.org/10.1111/1365-2745.13708

Chuine, I., 2000. A unified model for budburst of trees. Journal of *Theoretical Biology*, 207(3): 337–347. https://doi.org/10.1006/jtbi.2000.2178

Chuine, I., Kramer, K., Hänninen, H., 2003. Plant development models. In Schwartz, M.D.(eds). *Phenology: an integrative environmental science*. Tasks for VegetationScience,39.Dordrecht:Springer,p.217–235.https://doi.org/10.1007/978-94-007-0632-3_14

Fazilova, N.F., 2013. Fenologiya kashtana konskogo obyknovennogo (Aesculus hippocastanum) v Uzbekistane [Phenology of horse chestnut (Aesculus hippocastanum) in Uzbekistan]. *Aktualnye Napravleniya Nauchnyh Issledovanij XXI Veka: Teoriya i Praktika*, 4: 134–136. (In Russian).

Finn, G.A., Straszewski, A.E., Peterson, V., 2007. A general growth stage for describing trees and woody plants. *Annals of Applied Biology*, 151: 127–131. https://doi.org/ 10.1111/j.1744-7348.2007.00159.x

Flynn, D.F.B., Wolkovich, E.M., 2018. Temperature and photoperiod drive spring phenology across all species in a temperate forest community. *New Phytologist*, 219: 1353–1362. https://doi.org/10.1111/nph.15232

Forsythe, W.C., Rykiel, E.J.Jr., Stahl, R.S., Wu, H.-I., Schoolfield, R.M., 1995. A model comparison for daylength as a function of latitude and day of year. *Ecological Modelling*, 80 (1): 87–95. https://doi.org/10.1016/0304-3800(94)00034-F

Fu, Y.H., Piao, S., Zhou, X., Geng, X., Hao, F., Vitasse, Y., Janssens, I.A., 2019. Short photoperiod reduces the temperature sensitivity of leaf-out in saplings of Fagus sylvatica but not in horse chestnut. *Global Change Biology*, 25: 1696–1703. https://doi.org/10.1111/gcb.14599

Gauzere, J., Delzon, S., Davi, H., Bonhomme, M., de Cortazar-Atauri, I.G., Chuine, I., 2017. Integrating interactive effects of chilling and photoperiod in phenological process-based models. A case study with two European tree species: Fagus sylvatica and Quercus petraea. *Agricultural and Forest Meteorology*, 244–245: 9–20. https://doi.org/10.1016/j.agrformet.2017.05.011

Gauzere, J., Lucas, C., Ronce, O., Davi, H., Chuine, I., 2019. Sensitivity analysis of tree phenology models reveals increasing sensitivity of their predictions to winter chilling temperature and photoperiod with warming climate. *Ecological Modelling*, 411: 108805. https://doi.org/10.1016/j.ecolmodel.2019.108805

Ge, Q., Wang, H., Rutishauser, T., Dai, J., 2015. Phenological response to climate change in China: a meta-analysis, *Global Change Biology*, 21: 265–274. https://doi.org/10.1111/gcb.12648

Geng, X., Fu, Y.H., Piao, S., Hao, F., De Boeck, H.J., Zhang, X., Chen, S., Guo, Y., Prevéy, J.S., Vitasse, Y., Peñuelas, J., Janssens, I.A., Stenseth, N.Ch., 2022. Higher temperature sensitivity of flowering than leaf-out alters the time between phenophases across temperate tree species. *Global Ecology and Biogeography*, 31: 901–911. https://doi.org/10.1111/geb.13463

Hänninen, H., 1990. Modelling bud dormancy release in trees from cool and temperate regions. *Acta Forestalia Fennica*, 213: 1–47. https://doi.org/10.14214/aff.7660

Korsakova, S., Korzin, V., Plugatar, Y., Kazak, A., Gorina, V., Korzina, N., Khokhlov, S., Makoveichuk, K., 2023. Modelling of climate change's impact on Prunus armeniaca L.'s flowering time. *Inventions*, 8: 65. https://doi.org/10.3390/inventions8030065

Korsakova, S.P., Korsakov, P.B., Bagrikova, N.A., 2020. Climatogenic changes and forecast of blooming timing of Juniperus deltoides (Cupressaceae). *Science in the South of Russia*, 16 (3): 40–52. https://doi.org/10.7868/S25000640200305

Korzh, D.A., Trikoz, N.N., 2022. Vliyanie abioticheskih faktorov na sezonnuyu dinamiku chislennosti Cameraria ohridella Deschka & Dimic v Nikitskom Botanicheskom Sadu [The influence of abiotic factors on the seasonal dynamics of the abundance of Cameraria ohridella Deschka & Dimic in the Nikitsky Botanical Gardens]. *Biologiya Rastenij i Sadovodstvo: Teoriya, Innovacii*, 3 (164): 71–80. https://doi.org/10.36305/2712-7788-2022-3-164-71-80 (In Russian).

Kuranda, Yu.V., 2021. Semennaya reprodukciya Aesculus hippocastanum L. v kollekcii barnaulskogo dendrariya [Seed reproduction of Aesculus hippocastanum L. in the collection of the Barnaul arboretum]. *Trudy po Introdukcii i Akklimatizacii Rastenij*, 1: 583–588. (In Russian).

Lang, G., Early, J.D., Martin, G., Darnell. R., 1987. Endo-, para-, and ecodormancy: physiological terminology and classification for dormancy research. *Hort Science*, 22: 371–377. https://doi.org/10.21273/HORTSCI.22.5.701b

Laube, J., Sparks, T.H., Estrella, N., Höfler, J., Ankerst, D.P., Menzel, A., 2014. Chilling outweighs photoperiod in preventing precocious spring development. *Global Change Biology*, 20 (1): 170–182. https://doi.org/10.1111/gcb.12360

Malyshev, A.V., Henry, H.A.L., Bolte, A., Arfin Khan, M.A.S., Kreyling, J., 2018. Temporal photoperiod sensitivity and forcing requirements for budburst in temperate tree seedlings. *Agricultural and Forest Meteorology*, 248: 82–90. https://doi.org/10.1016/j.agrformet.2017.09.011

Meng, L., Zhou, Y., Gu, L., Richardson, A.D., Peñuelas, J., Fu, Y., Wang, Y., Asrar, G.R., De Boeck, H.J., Mao, J., Zhang, Y., Wang, Zh., 2021. Photoperiod decelerates the advance of spring phenology of six deciduous tree species under climate warming, *Global Change Biology*, 27: 2914–2927. https://doi.org/10.1111/gcb.15575

Migliavacca, M., Sonnentag, O., Keenan, T.F., Cescatti, A., O'Keefe, J., Richardson, A.D., 2012. On the uncertainty of phenological responses to climate change, and implications for a terrestrial biosphere model. *Biogeosciences*, 9: 2063–2083. https://doi.org/10.5194/bg-9-2063-2012

Minin, A.A., Ananin, A.A., Buyvolov, Yu.A., Larin, E.G.,

Lebedev, P.A., Polikarpova, N.V., Prokosheva, I.V., Rudenko, M.I., Sapelnikova, I.I., Fedotova, V.G., Shuyskaya, E.A., Yakovleva, M.V., Yantser, O.V., 2020. Rekomendacii po unifikacii fenologicheskih nablyudenij v Rossii [Recommendations to unify phenological observations in Russia]. *Nature Conservation Research*, 5 (4): 89–110. https://dx.doi.org/10.24189/ncr.2020.060. (In Russian).

Minin, A.A., Ran'kova, E.Ya., Ribina, E.G., Buyvolov, U.A., Sapel'nikova, I.I., Filatova, T.D., 2016. Fenoindikaciya izmenenij klimata za period 1976–2015 gg. v central'noj chasti Evropejskoj territorii Rossii [Phenoindication of current fluctuations in climate in the centre of the European part of Russia for the 1976–2015 years]. *Problemy Ekologicheskogo Monitoringa i Modelirovaniya Ekosistem*, 27 (2): 17–28. https://doi.org/10.21513/0207-2564-2016-2-17-28. (In Russian).

Mo, Y., Li, X., Guo, Y., Fu, Y., 2023. Warming increases the differences amongst spring phenology models under future climate change. *Frontiers in Plant Science*, 14: 1266801. https://doi.org/10.3389/fpls.2023.1266801

Olsson, C., Olin, S., Lindström, J., Jönsso, A.M., 2017. Trends and uncertainties in budburst projections of Norway spruce in Northern Europe. *Ecology and Evolution*, 7: 9954–9969. https://doi.org/10.1002/ece3.3476

Ovaskainen, O., Meyke, E., Lo, C., et al., 2020. Chronicles of nature calendar, a long-term and large-scale multitaxon database on phenology. *Scientific Data*, 7: 47. https://doi.org/10.1038/s41597-020-0376-z

Parmesan, C., 2007. Influences of species, latitudes and methodologies on estimates of phenological response to global warming. *Global Change Biology*, 13(9): 1860–1872. https://doi.org/10.1111/j.1365-2486.2007.01404.x

Polgar, C., Primack, R.B., 2011. Leaf-out phenology of temperate woody plants: from trees to ecosystems. *New Phytologist*, 191: 926–941. https://doi.org/10.1111/j.1469-8137.2011.03803.x

R Core Team, 2022. *R: a language and environment for statistical computing*. R Foundation for Statistical Computing, Vienna, Austria. https://cran.r-project.org/.

Richardson, A.D., Keenan, T.F., Migliavacca, M., Ryu, Y., Sonnentag, O., Toomey, M., 2013. Climate change, phenology, and phenological control of vegetation feedbacks to the climate system. *Agricultural and Forest Meteorology*, 169: 156–173. https://doi.org/10.1016/j.agrformet.2012.09.012

Shvydenko, I.M., Bulat, A.G., Slyusarchuk, V.E., Nazarenko, V.V., Buhaiov, S.M., Cherkis, T.M., Stankevych, S.V., Zabrodina, I.V., Matsyura, A.V., 2021. Seasonal development of the chestnut leaf miner (Cameraria ohridella Deschka & Dimic, 1986) in the eastern forest-steppe of Ukraine. *Ukrainian Journal of Ecology*, 11 (2): 407–416. https://doi.org/10.15421/2021_130

Templ, B., Koch, E., Bolmgren, K., Ungersböck, M., Paul, A., Scheifinger, H., Rutishauser, Th., Busto, M., Chmielewski, F.-M., Hájková, L., Hodzić, S., Kaspar, F., Pietragalla, B., Romero-Fresneda, R., Tolvanen, A., Vučetič, V., Zimmermann, K., Zust, A., 2018. Pan European Phenological database (PEP725): a single point of access for European data. *International Journal of Biometeorology*, 62: 1109–1113. https://doi.org/10.1007/s00484-018-1512-8

Wang, S., Wu, Z., Gong, Y., Wang, S., Zhang, W., Zhang, Sh., De Boeck, H.J., Fu, Y.H., 2022. Climate warming shifts the time interval between flowering and leaf unfolding depending on the warming period. *Science China Life Sciences*, 65: 2316–2324. https://doi.org/10.1007/s11427-022-2094-6

Wickham, H., 2016. *ggplot2*: *elegant graphics for data analysis*. New York: Springer-Verlag. https://ggplot2.tidyverse.org.

Wolkovich, E.M., Cook, B.I., Allen, J.M., Crimmins, T.M., Betancourt, J.L., Travers, S.E., Pau, S., Regetz, J., Davies, T.J., Kraft, N.J., Ault, T.R., Bolmren, K., Mazer, S.J., McCabe, G.J., McGill, B.J., Parmesan, C., Salamin, N., Schwartz, M.D., Cleland, E.E., 2012. Warming experiments under predict plant phenological responses to climate change. *Nature*, 485 (7399): 494–497. https://doi.org/10.1038/nature11014

Zohner, C., Benito, B., Svenning, J-C., Renner, S.S., 2016. Day length unlikely to constrain climate-driven shifts in leaf-out times of northern woody plants. *Nature Climate Change*, 6: 1120–1123. https://doi.org/10.1038/nclimate3138

Zohner, C.M., Renner, S.S., 2015. Perception of photoperiod in individual buds of mature trees regulates leaf-out. *New Phytologist*, 208: 1023–1030. https://doi.org/10.1111/nph.13510

Received June 2, 2024
Accepted December 6, 2024

Supplementary material

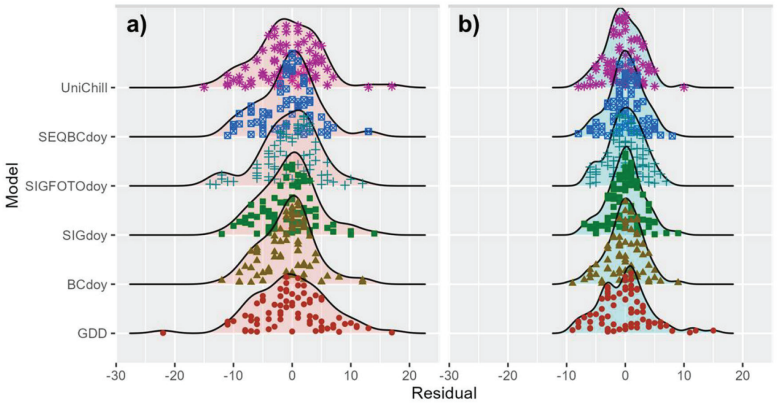

Fig. S1. Histogram of prediction errors for: a) leaf unfolding and b) full flowering date from phenological models for *A. hippocastanum* in the SCC for the period of 1931–2022.

Table S1. Model equations for the prediction of the leaf unfolding and full flowering dates of horse chestnut

Model	Equation	Fitting parameters
GDD	$Sf_t = \sum_{t1}^{t_2} \begin{cases} 0, & T_t < T_b \\ T_t - T_b, & T_t \geq T_b \end{cases}$, where $Sf_{t2} = F^*$	T_b,F*; t_1=1 January
BCdoy	$Sf_t = \sum_{t1}^{t_2} \begin{cases} 0, & T_t < T_b \\ (T_t - T_b) \cdot \left(\frac{DL}{10}\right)^{EXPO} & T_t \geq T_b \end{cases}$, where $S_{ft2} = F^*$	T_b,*EXPO*, F^*, t_1
SIGdoy	$Sf_t = \sum_{t_1}^{t_2} \frac{1}{1 + e^{b_f(T_t - c_f)}}$, where $S_{ft2} = F^*$	b_f,c_f,F^*,t_1
FOTOdoy	$Sf_t = \sum_{t_1}^{t_2} \left[\frac{1}{1 + e^{b_f(T_t - c_f)}} \times \left(\frac{DL}{10}\right)^{EXPO}\right]$, where $S_{ft2} = F^*$	b_f,c_f, *EXPO*, F^*,t_1
SEQBCdoy	$Sc_t = \sum_{t_0}^{t_1} \begin{cases} 0, & T_t \leq -3.4 \text{ или } T_t \geq 10.4 \\ \frac{T_t - (-3.4)}{T_{opt} - (-3.4)}, & -3.4 < T_t \leq T_{opt} \\ \frac{T_t - 10.4}{T_{opt} - 10.4}, & T_{opt} < T_t < 10.4 \end{cases}$, where $S_{ct1} = C^*$ $Sf_t = \sum_{t_1}^{t_2} \begin{cases} 0, & T_t < T_b \\ (T_t - T_b) \cdot \left(\frac{DL}{10}\right)^{EXPO} & T_t \geq T_b \end{cases}$, where $S_{ft2} = F^*$	T_{opt}, C^*; t_0= 1 November T_b,*EXPO*,F^*,t_1
UniChill	$Sc_t = \sum_{t_0}^{t_1} \frac{1}{1 + e^{a_c(T_t - c_c)^2 + b_c(T_t - c_c)}}$, where $S_{ct1} = C^*$ $Sf_t = \sum_{t_1}^{t_2} \frac{1}{1 + e^{b_f(T_t - c_f)}}$, where $S_{ft2} = F^*$	a_c, b_c, c_c, C^*; t_0=1 December b_f,c_f,F^*, t_1

t0, *t1* and *t2*, starting dates of chilling, forcing unit accumulation and phenoevent onset, respectively. T_{opt}, optimal chilling temperature (°C). T_b, threshold of daily mean air temperature for forcing unit accumulation (°C). C^*, chilling unit requirement (CU). F^*, forcing unit requirement (FU). a_c,b_c,c_c,b_f,c_f, empirical parameters of the sigmoidal function (c, chilling, f, forcing). *EXPO*, exponential constant for relating forcing accumulation to day length.

Table S2. Geographical locations of phenological observation sites

Country, region	Site	Longitude (°N)	Latitude (°E)	Altitude (m a.s.l.)	Years
Uzbekistan	Tashkent	41.311	69.280	480	1976–1980 2011–2012
Crimea	Yalta	44.510	34.240	190	1931–2022
Bosnia and Herzegovina	Bihac	44.800	15.867	246	1976–1989
Croatia	Daruvar	45.600	17.233	161	2011–2015
Croatia	Zagreb	45.817	16.033	121	2005–2015
Croatia	Krizevci	46.033	16.550	138	2011–2015
Switzerland	Adelboden	46.500	7.567	1,350	1991–1992 2002–2006
France	Segre-en-Anjou Bleu	47.681	−0.872	31	2012–2018
Slovakia	Kravany nad Dunajom	47.767	18.483	110	2000–2013
Slovakia	Slanské Nové Mesto	48.633	21.517	250	2000–2013
Slovakia	Hranovnica	48.983	20.317	620	2000–2013
Ukraine	Kyiv	49.744	31.456	138	1973–2016
Ukraine	Kharkiv	50.000	36.224	155	1961 2008–2012
England	Bournemouth	50.783	−1.883	32	2002–2005
Russia	Kursk	51.147	36.430	226	1963–2014
Russia	Bryansk	53.243	34.364	216	2014–2015
Germany	Marnitz	53.317	11.933	85	2009–2015
Russia	Barnaul	53.347	83.777	159	2019–2020
Belarus	Braslavskie Ozera	55.596	27.054	127	2008–2015

Table S3. Geographical locations of weather stations

Country, region	Site	Longitude (°N)	Latitude (°E)	Altitude (m a.s.l.)	Years
Uzbekistan	Tashkent	41. 267	69. 267	488	1975–1980 2010–2012
Crimea	Yalta	44. 510	34.240	207	1930–2022
Bosnia and Herzegovina	Bihac	44. 817	15.883	246	1975–1989
Croatia	Daruvar	45.600	17.200	161	2010–2015
Croatia	Zagreb	45.867	16.033	123	2004–2015
Croatia	Krizevci	46.033	16.556	155	2010–2015
Switzerland	Adelboden	46.500	7.560	1,320	1990–1992 2001–2006
France	Segre-en-Anjou Bleu (Angers weather station)	47.473	−0.556	48	2011–2018
Slovakia	Hurbanovo	47.867	18.200	115	1999–2013
Slovakia	Kosice	48.669	21.241	231	1999–2013
Slovakia	Poprad-Tatry	49.067	20.250	694	1999–2013
Ukraine	Kyiv	50.400	30.567	167	1972–2016
Ukraine	Kharkiv	49.967	36.133	155	1960–1961 2008–2012
England	Bournemouth	50.783	−1.833	11	2002–2005
Russia	Kursk	51.767	36.167	246	1962–2014
Russia	Bryansk	53.250	34.317	214	2013–2015
Germany	Marnitz	53.317	11.933	80	2008–2015
Russia	Barnaul	53.433	83.517	183	2018–2020
Belarus	Braslavskie Ozera (Daugavpils weather station)	55.867	26.500	122	2007–2015